Supporting Information

Plasticizer and Catalyst Co-Functionalized PEDOT:PSS Enables Stretchable Electrochemical Sensing of Living Cells

Jing Yan,[a] Yu Qin,[a] Wen-Ting Fan,[a] Wen-Tao Wu,[a] Song-Wei Lv,[b] Li-Ping Yan,[a] Yan-Ling Liu[a] and Wei-Hua Huang*[a]*

a. College of Chemistry and Molecular Sciences, Wuhan University, Wuhan 430072, China.

b. School of Pharmacy, Changzhou University, Changzhou 213164, China.

E-mail: yanlingliu@whu.edu.cn; whhuang@whu.edu.cn.

Supporting Figures

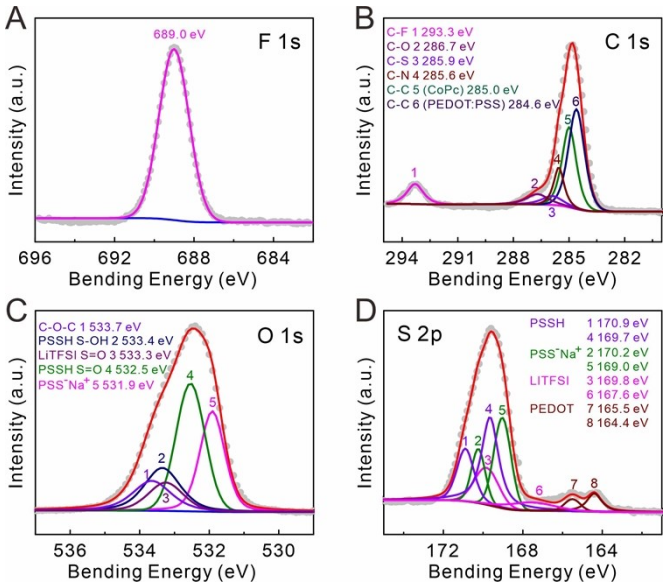

Figure S1. XPS spectra of (A) F 1s state, (B) C 1s state, (C) O 1s state, (D) S 2p state.

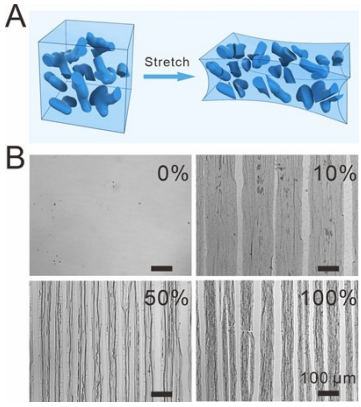

Figure S2. (A) Schematic illustration showing the stretchability principle of PP film. (B) Optical microscope images of PP/PDMS film recovering from being submitted to various strains.

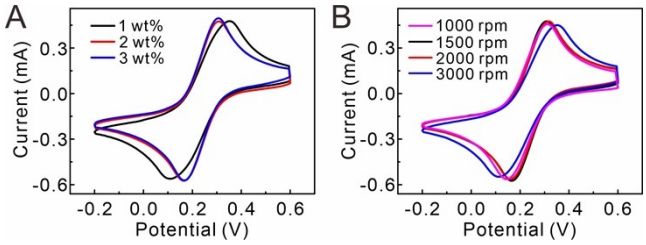

Figure S3. (A) CVs of PPL/PDMS films with different contents of LiTFSI at the spin-coating speed of 1500 rpm obtained in 10 mM $K_3[Fe(CN)_6]$. (B) CVs of PPL/PDMS films using different spin-coating speeds with 2 wt% LiTFSI obtained in 10 mM $K_3[Fe(CN)_6]$.

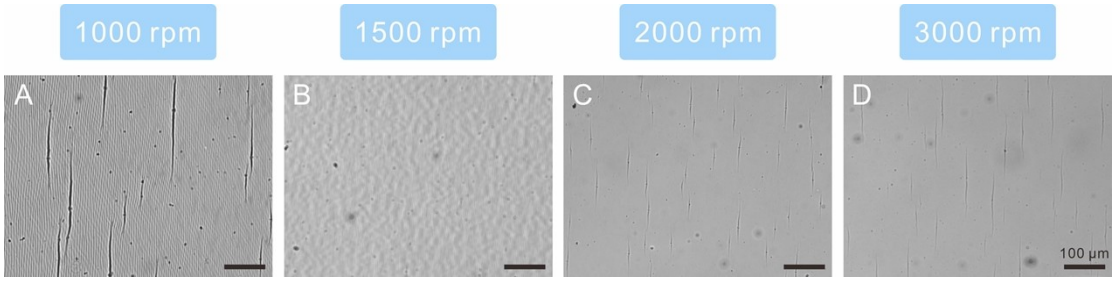

Figure S4. Optical microscope images of PPL/PDMS films with 2 wt% LiTFSI at different spin-coating speeds recovering from being stretched to a strain of 50%.

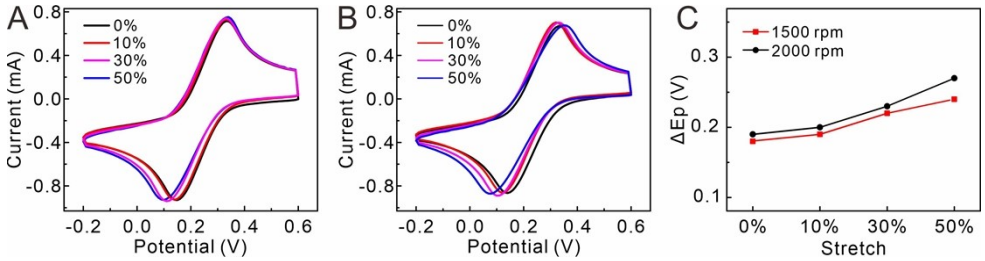

Figure S5. CVs of PPL/PDMS films with 2 wt% LiTFSI at a spin-coating speed of (A) 1500 rpm and (B) 2000 rpm obtained in 10 mM $K_3[Fe(CN)_6]$ after being stretched to different tensile strains. (C) Potential differences of CVs obtained in 10 mM $K_3[Fe(CN)_6]$ of PPL/PDMS films with 2 wt% LiTFSI at different spin-coating speeds under different strains.

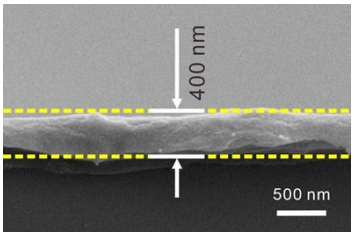

Figure S6. SEM image of the cross section of PPLC film.

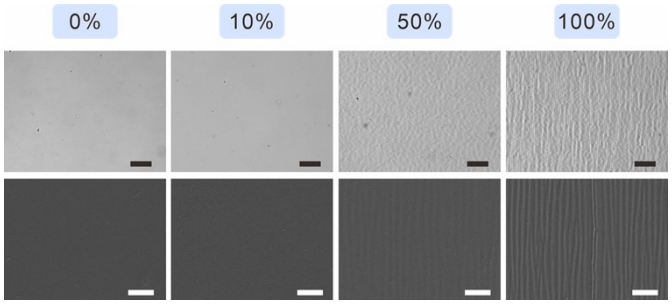

Figure S7. Optical microscope (top row) and SEM (bottom row) images of PPL/PDMS film recovering from being submitted to various strains. Scale bar: 100 μm (black) and 10 μm (white).

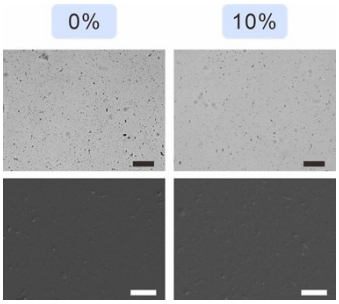

Figure S8. Optical microscope (top row) and SEM (bottom row) images of PPLC/PDMS film recovering from being submitted to various strains. Scale bar: 100 μm (black) and 10 μm (white).

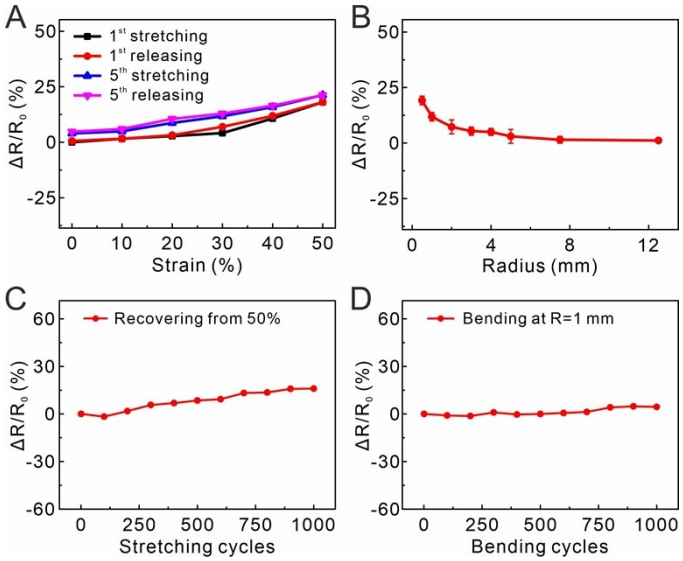

Figure S9. Relative difference in resistance of PPLC/PDMS as a function of (A) tensile strains (0~50%) in the first and fifth stretch-releasing and (B) various bending radii (from 0.5 mm to 12.5 mm, data presented as mean ± SEM, n = 3). (C, D) Relative difference in resistance of PPLC/PDMS during cyclic deformations.

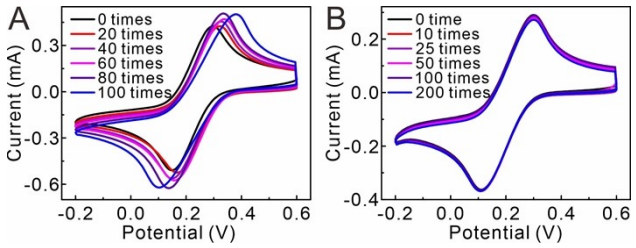

Figure S10. CVs of PPLC/PDMS obtained in 10 mM $K_3[Fe(CN)_6]$ after recovering from being (A) stretched to 50% and (B) bended at a radius of 3 mm for different times.

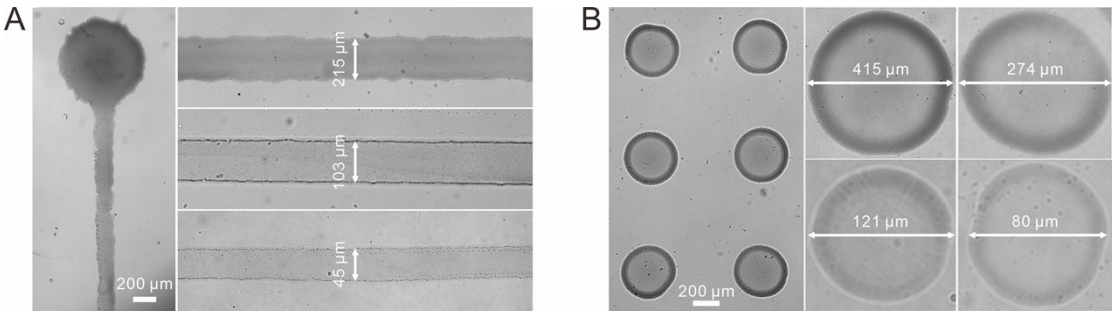

Figure S11. Optical microscope images of PPLC with controllable sizes obtained by photolithography (A) and inkjet printing (B).

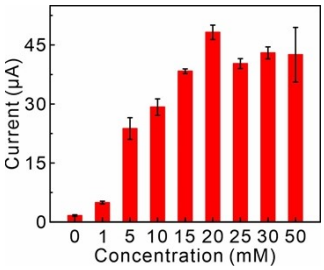

Figure S12. Statistical results of the current responses to 1 mM H_2O_2 at the peak potential of +0.55 V (vs Ag/AgCl) of CVs of PPLC/PDMS films with different contents of CoPc (data presented as mean ± SEM, n = 3).

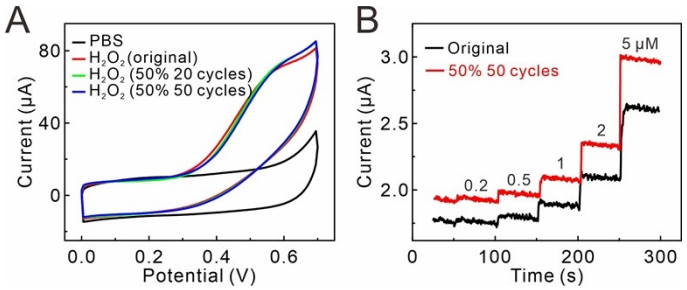

Figure S13. CV responses of PPLC/PDMS electrode in 1 mM H_2O_2 (A) and amperometric responses of PPL/PDMS electrode to H_2O_2 at a potential of +0.55 V (vs. Ag/AgCl) to increasing H_2O_2 concentrations (B) before and after recovering from being repeatedly stretched to a strain of 50%.

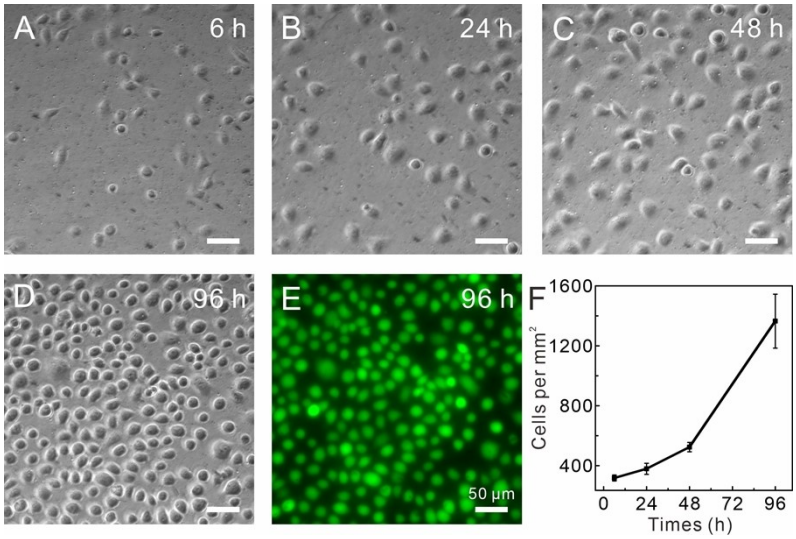

Figure S14. (A-D) The microscopic images of 16HBECs cultured on PPLC/PDMS film for different times. (E) Fluorescent microscopic image of 16HBECs stained with Calcein-AM (green) and PI (red) after cultured on PPLC/PDMS film for 96 h. (F) Proliferation curve of 16HBECs cultured on PPLC/PDMS film (data presented as mean ± SEM, n = 5).

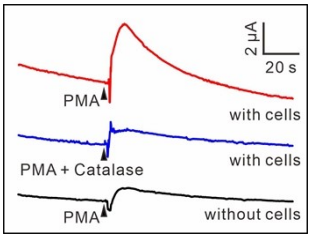

Figure S15. Amperometric responses detected from 16HBECs under stimulation of 50 μM PMA.

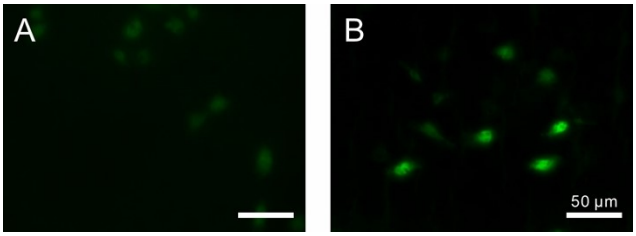

Figure S16. Fluorescence microscopic images of 16HBECs cultured on PPLC/PDMS film (A) without strain and (B) with a strain of 30% stained by DCFH-DA.

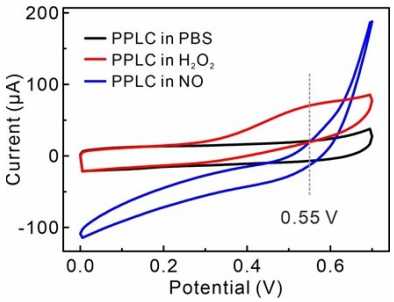

Figure S17. CVs of PPLC/PDMS electrodes in the PBS solution with and without 1 mM H_2O_2 or NO.